

Applying artificial snowfalls to reduce the melting of the Muz Taw Glacier, Sawir Mountains

Feiteng Wang^{1*}, Xiaoying Yue¹, Lin Wang¹, Huilin Li¹, Zhencai Du², Jing Ming³

1 State Key Laboratory of Cryospheric Sciences / Tien Shan Glaciological Station, Northwest Institute of Eco-Environment and Resources, Chinese Academy of Sciences, Lanzhou 730000, China

2 Center for Monsoon System Research, Institute of Atmospheric Physics, Chinese Academy of Sciences, Beijing 100029, China

3 Beacon Science & Consulting, Doncaster East, VIC 3109, Australia

Correspondence

* Feiteng Wang, wangfeiteng@lzb.ac.cn

1 **ABSTRACT**

2 The glaciers in the Sawir Mountains, Altai area, have been experiencing a continuing
3 and accelerating ice loss since 1959, although the snowfall here is abundant and
4 evenly distributed over the year. As an attempt to reduce their melting, we carried
5 out two artificial-snowfall experiments to the Muz Taw glacier during 19 – 22 Aug
6 2018. We measured the albedo and mass balance at different sites along the glacier
7 before and after the experiments. Two automatic weather stations (AWS) were set
8 up at the equilibrium line altitude (ELA) of the glacier as the target area and the
9 forefield as the control area to record the precipitations, respectively. The
10 comparison of the two precipitation records from the two AWSs suggests that natural
11 precipitation could account for up to 21% of the snowfall received by the glacier
12 during the experiments. Because of the snowfalls, the glacier's surface albedo
13 significantly increased in the mid-upper part; the average mass loss decreased by 32
14 to 41 mm w.e. after the experiments (Aug 18 – 24) comparing to that before (Aug 12
15 – 18); and the mass resulting from the snowfalls accounted for 42% to 54% of the
16 total melt during Aug 18 – 24. We also propose a mechanism involving artificial
17 snowfall, albedo and mass balance and the feedbacks, describing the role of
18 snowfall in reducing the melting of the glacier. The work in current status is primitive
19 as a preliminary trial in science and engineering, the conclusions of which need more
20 controlling experiments to validate in larger spatial and temporal scales in future.

21

22 **Keywords**

23 artificial snowfall, Muz Taw Glacier, Sawir Mountains, glacier mass balance, reduce
24 melting

25

26 **1 Introduction**

27 Mountain glaciers are an essential part of the cryosphere. As high-altitude reservoirs,
28 they are vital solid-water resources (Immerzeel et al., 2019; Immerzeel et al., 2010).
29 Glacier fluctuations represent an integration of changes in the mass and energy
30 balance and are well recognized as high-confidence indicators of climate change
31 (Bojinski et al., 2014). Satellite and in-situ observations of changes in the glacial
32 area, length and mass show a global coherence of continued mountain-glacier
33 recession in the last three decades with only a few exceptions (Zemp et al., 2019).
34 For the Sawir Mountains, the ablation of the glaciers is more intense than the global
35 average, and the total area of the glaciers reduced by 46% from 23 km² in 1977 to
36 12.5 km² in 2017 (Wang et al., 2019). The accelerated retreat of glaciers not only
37 causes spatial and temporal changes in water resources but also has a significant
38 impact on sea-level rise, regional water cycles, ecosystems and socio-economic
39 systems (such as agriculture, hydropower and tourism); the melting of glaciers also
40 increases the occurrence of glacial disasters, such as glacial lake outburst flooding,
41 icefalls and glacial debris flows (Hock et al., 2019). And the ski resorts around
42 Grenoble in France have been encountering the declining snow reliability since the
43 1960s (Gerbaux et al., 2020).

44

45 So far, there are not so many approaches used in practice for reducing the rate of
46 glacier ablation. Some administrative measures, including energy conservation,
47 temperature-increase control and establishing glacial reserves, have been taken to
48 reduce the ice melting on Earth. In recent years, new ideas and techniques have
49 emerged for slowing the melting of glaciers. For example, in the Rhone glacier of the
50 Swiss Alps, white blankets are used to shelter the glacier and slow down its melting
51 (Dyer, 2019). In the Morteratsch Glacier of the Alps, artificial snow was expected to
52 be applied for slowing down the glacier melting (Oerlemans et al., 2017). In Austrian
53 glacier ski resorts, over 20-m thickness of the ice was preserved on mass balance
54 managed areas compared to non-maintained areas during 1997 – 2006 (Fischer et
55 al., 2016).

56

57 A peer review report on global artificial-snowfall activities by the World
58 Meteorological Organization suggests that the toxicity of the seeding material
59 (majorly silver iodine, i.e. AgI) is unlikely to trigger environmental hazards

60 (Flossmann et al., 2018). A potential concern is that artificial-precipitation activities
61 might redistribute the natural precipitation over a region; however, applying cloud
62 seeding over the mountain glaciers usually up to 5 km in length in Central Asia, is
63 presumably acceptable.

64

65 There have always been controversial discussions on the virtual efficacy and
66 positiveness of using AgI smoke to seed cloud and enhancing precipitations since
67 the measure was introduced by Vonnegut (1947). The controversy mainly resides in
68 two sides. One side claimed that no statistical or physical evidence had been
69 provided to establish the scientific validity of the operations (Council, 2003;
70 Silverman, 2001), while the other affirmed that the past operations conducted in
71 Australia successfully increased precipitations by 5% up to 50% (Bowen, 1952;
72 CSIRO, 1978; Smith, 1967). However, both sides agreed that the experiments of
73 seeding clouds and producing more precipitation were promising and deserved more
74 observations to understand the link of physical reactions leading to precipitation
75 (Council, 2003).

76

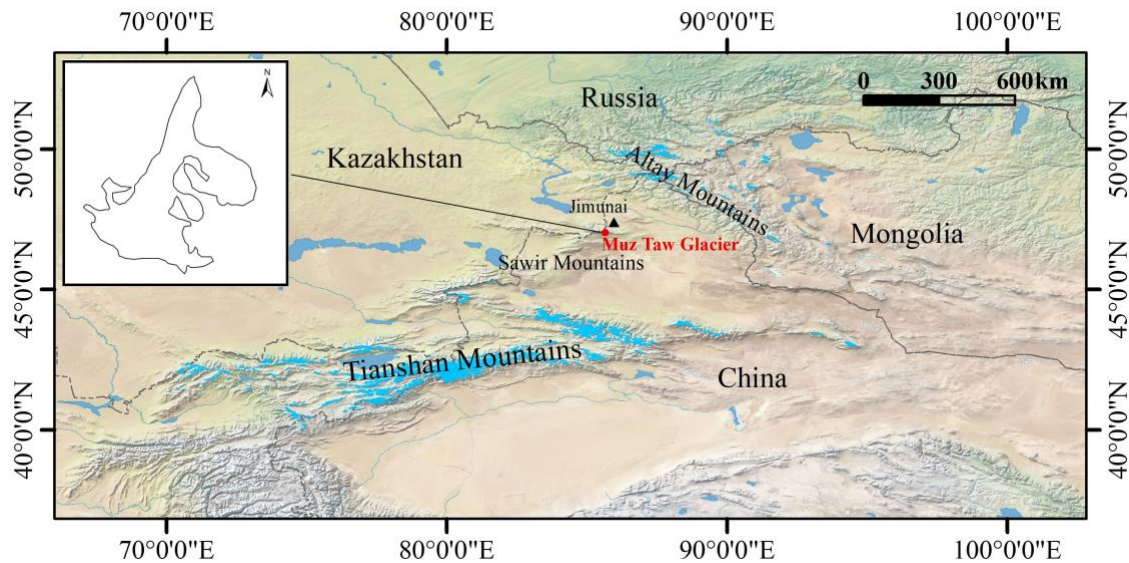
77 As an attempt in science and engineering, we select the Muz Tau glacier in the
78 Sawir Mountains as the projected glacier. During the glacier's ablation period in
79 2018, we tried to induce artificial precipitations by using the ground AgI smoke
80 generators to seed clouds over the glacier. These smog generators were set up
81 there by the local meteorological service for artificial-precipitation tasks. We also
82 combined the precipitation amounts and type, time and frequency recorded by the
83 rainfall gauge and the mass balance and albedo of the glacier measured to study the
84 role of artificial snowfall in reducing the mass loss of the glacier.

85

86 **2 The Sawir Mountains and the Muz Taw Glacier**

87 The Sawir Mountains span the border shared by China and Kazakhstan and are the
88 transitional section between the Tianshan Mountains and the central Altay
89 Mountains. The Muz Taw Glacier (47°04'N, 85°34'E) is a northeast-orientated valley
90 glacier with an area of 3.13 km² and a length of 3.2 km in 2016, located on the
91 northern side of the Sawir Mountains (Figure 1). Its elevation from the terminus to

92 the highest point ranges from 3137 m to 3818 m a.s.l. and its ice volume is 0.28 km³,
93 with an average ice thickness of 66 m (Wang et al., 2018).



94
95 *Figure 1 Location of the Muz Taw glacier and the Sawir Mountains, where the map in the background*
96 *is downloaded from the website <https://www.natureearthdata.com/> and the outline of the glacier is*
97 *sourced in Guo et al. (2015).*
98

99 The general circulation over the study area is featured by the prevailing westerlies
100 interacting with the Asian anticyclone and polar air mass in winter (Panagiotopoulos
101 et al., 2005). At the Jimunai Meteorological Station (984 m a.s.l.), 46 km northeast of
102 the Muz Taw Glacier, the annual mean air temperature measured was 4.27 °C; the
103 annual mean precipitation was 212 mm during 1961–2016, and the winter
104 precipitation accounted for 10% - 30% of the annual total.

105
106 The Muz Taw Glacier has been in constant recession since 1959 (Wang et al.,
107 2019). Especially for the past 20 years, it has been experiencing a rapid and
108 accelerated shrinkage. From 1977 to 2017, the glacier area decreased by 10.51 km²,
109 accounting for 45.72 % of its previous surface area (Wang et al., 2019). The average
110 retreat rate of the glacier terminus was 11.5 m a⁻¹ during 1989 – 2017. The latest
111 measurements show the mass balance of the Muz Taw Glacier was – 975 mm w.e.
112 in 2016, – 1192 mm w.e. in 2017 and – 1286 mm w.e. in 2018, respectively; and the
113 annual equilibrium line of the glacier was approximately 3400 m a.s.l. (Song, 2019).

114 115 **3 Field Experiments and measurements**

116 **3.1 Artificial-precipitation experiment**

117 We used a WR-08X digital radar system (Wuxi Leyoung Electronics Technology Co.,
118 Ltd) built up at the Jimunai Meteorological station to identify the precipitation clouds
119 around the Sawir Mountains. The radar is a new X-band digital weather radar
120 capable of detecting meteorological targets within 300 km. The radar can
121 quantitatively detect the spatial distribution of intensity of cloud rain targets below 20
122 km distanced from 5 km to 150 km and their motions (e.g., developing height,
123 moving direction and speed.). It can also provide real-time meteorological
124 information. A more detailed description of its application in this area can be referred
125 to in Xu et al. (2017).

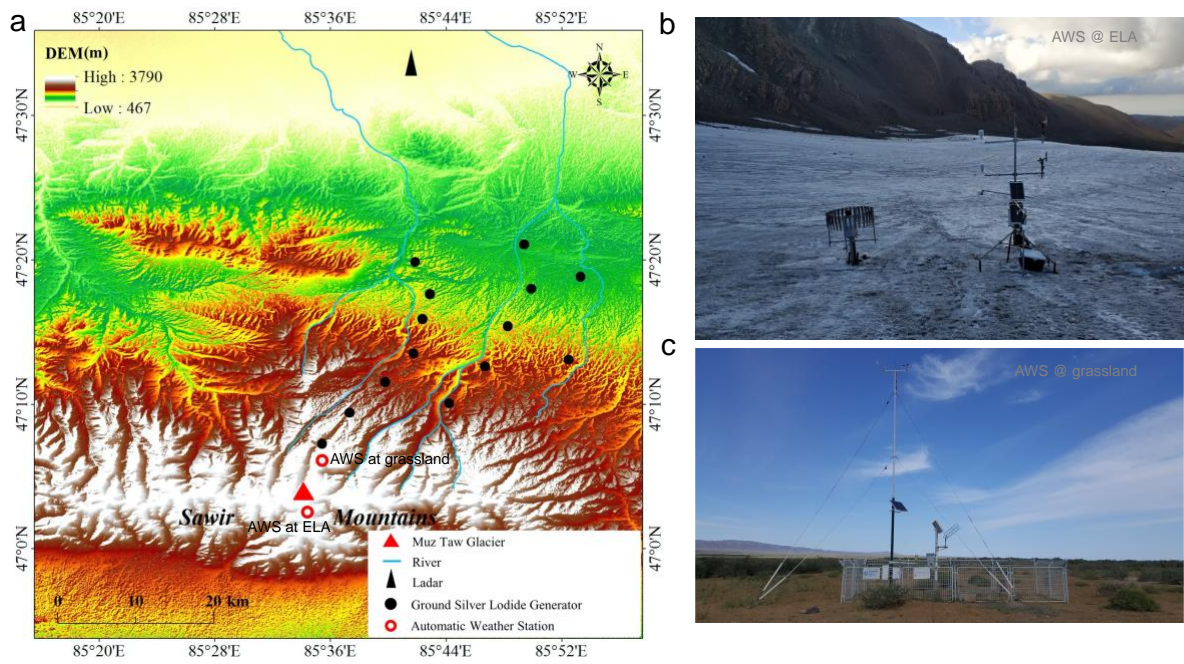
126

127 The Muz Taw glacier is developing along the valley, and the terminal is the heading
128 source of the Ulequin Urastu River and Ulast River. We distributed 14 silver-iodide
129 (AgI) smog generators along the rivers. These smog generators use solar power to
130 light and are remotely controlled. The AgI sticks used in the generators allow to
131 generate 10^{14} AgI-contained ice nuclei per gram at $-7.5\text{ }^{\circ}\text{C} \sim -20\text{ }^{\circ}\text{C}$ (Kong et al.,
132 2016). In the daytime, valley winds prevail along the valley up to the glacier due to
133 intense radiation and the heating-and-lifting effect for air over the snow surface. It is
134 ideal for generating AgI smogs and carrying them by the upwards air stream over the
135 glacier surface to form precipitations. No extra water is needed to form precipitations
136 in our experiments. We monitored the distribution and structural developing of clouds
137 and identified the orientation, height and distance of the clouds approaching the
138 glacier at the radar station. Associated with observing the moving of the potential
139 target clouds and the receiving of the reflection of the radar transmission, we ignited
140 the smog generators for seeding artificial precipitations, when we realized the
141 possibility is high enough to form precipitation potentially (Figure 2). The detailed
142 operation of conducting artificial precipitations in the studied glacier has been
143 described in Xu et al. (2017).

144

145 First, we used the radar to identify local convective clouds in the background
146 synoptic clouds and measured the orientation, height and distance of the
147 convections for determining the time and area for performing artificial precipitation
148 seeding. And then we chose most favourable timing to ignite the silver-iodide smog
149 generators (Figure 3a) and let the silver-iodide (AgI) particles as catalyzer help

150 forming amounts of artificial ice nuclei (Figure 3b) to absorb more water vapour and
 151 promote to form precipitations.



152
 153 *Figure 2 a) The map of the study area, including the Muz Taw glacier, the two automatic weather*
 154 *stations (AWS) set up at the equilibrium line elevation (ELA) and the forefield of the glacier and the*
 155 *distribution of the silver-iodide-smog generators along the Ulequin Urastu River and Ulast River in the*
 156 *Sawir Mountains for seeding artificial precipitations, b) the AWS set up at the ELA and c) the AWS set*
 157 *up at the grassland with a straight distance of ~5 km north to the AWS at the ELA.*

158



159
 160 *Figure 3 a) Igniting the AgI smog generators along the terminal river when the cloud accumulated late*
 161 *on the afternoon of 19 and 22 Aug 2018, and b) the accumulating of clouds in the valley of the Muz*
 162 *Taw Glacier favoured by the AgI particles moved up towards the summit of the glacier.*

163

164 **3.2 Measurement by the automatic weather stations (AWS)**

165 We set up an automatic weather station (AWS at ELA) on a relatively flat surface
 166 near the equilibrium line altitude (ELA) of the Muz Taw glacier since 8 Aug 2018 (47°
 167 03'36"N, 85°33'43"E, 3430 m a. s. l.; Figure 2a&b and Figure 4). The AWS has

168 various sensors to fulfil the requirement of our study (Table 1). A thermometer
 169 (Pt100 RTD, ± 0.1 K) was mounted horizontally 1.5 m above the surface to measure
 170 air temperature. The measurement of albedo was calculated by measuring incoming
 171 and reflected shortwave radiation with the CNR4 pyranometer mounted on the AWS
 172 at the height of 1.5 m. The error of pyranometer is smaller than 1% in the wavelength
 173 from 0.3 μm to 2.8 μm . Precipitation was measured by an auto-weighing gauge (T-
 174 200B, Geonor Inc.) with an accuracy of about $\pm 0.1\%$. All sensors were connected to
 175 a data logger (CR6, Campbell) which is able to work in low temperature (-55 $^{\circ}\text{C}$) and
 176 record the hourly means every ten seconds. In the forefield of the glacier around five
 177 kilometers north of the AWS at the ELA, another AWS on the grassland (AWS at
 178 grassland) was set up by the local meteorological service to monitor conventional
 179 meteorology (Figure 2a&c).

180

181 *Table 1 The sensors mounted on the AWS and their technic features*

| Sensor | Measurement | Model | Accuracy or features |
|---------------------|----------------|---------------------|---------------------------------|
| Thermometer | temperature | Pt100 RTC | ± 0.1 K |
| Pyranometer | radiation | CNR4 | < 1% in 0.3 - 2.8 μm |
| Auto-weighing gauge | precipitation | T-200B, Geonor Inc. | $\pm 0.1\%$ |
| Data logger | data recording | CR6, Campbell | working in low temperature |

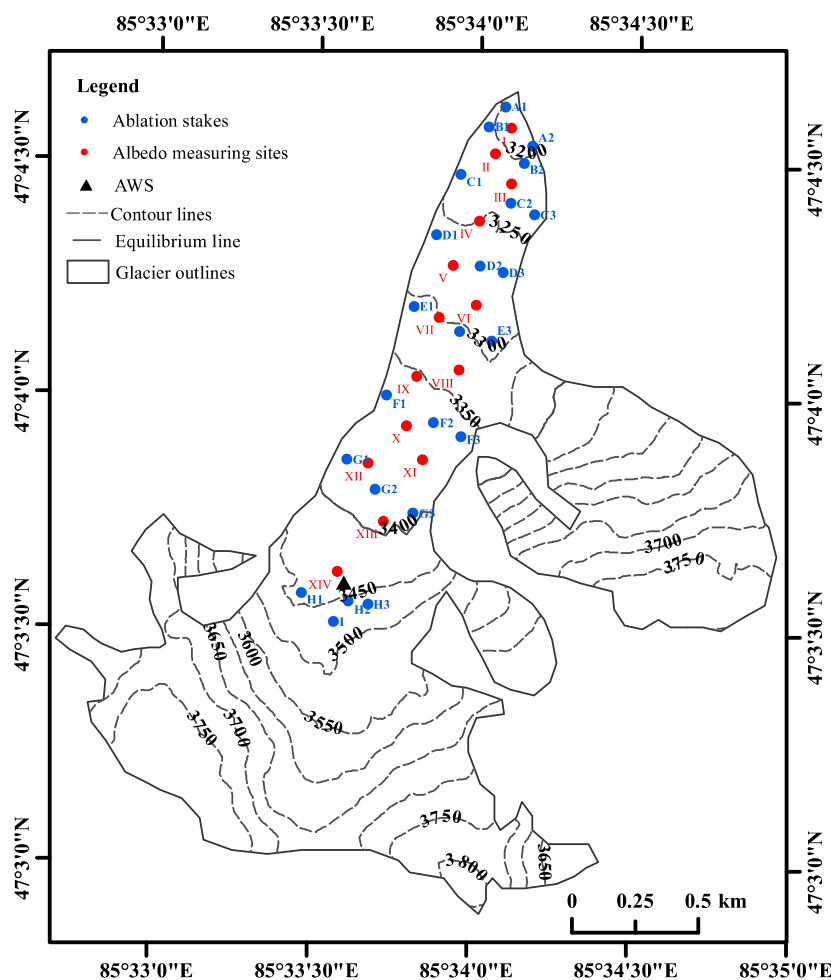
182

183 **3.3 Measurement of the surface spectral reflectance**

184 We used an ASD Fieldspec HandHeld 2 Spectroradiometer to measure the
 185 reflectance data at 325-1075 nm by with a resolution of 3 nm and an error of less
 186 than 4%. The measurement sensor fitted with a bare fibre was mounted on a tripod
 187 at 0.5 m above the surface and had a 25° field of view to a spot sized ~ 0.225 m in
 188 diameter. The spectroradiometer was calibrated to hemispherical atmospheric
 189 conditions at the time, by viewing white-reference panel and then viewing the glacier
 190 surface. We recalibrated the instrument on occasion when the sky radiation
 191 conditions changed. To minimize the influence of slope and solar zenith angle on
 192 albedo, we conducted the measurements in a water-level plane within 12:00-16:00
 193 local time. At each sampling site, three consecutive spectra consisting of ten dark
 194 currents per scan and ten white reference measurements were recorded and
 195 averaged. Meanwhile, cloud cover and surface type were noted for each
 196 measurement.

197

198 We measured spectral reflectance at fourteen sites across the glacier, on 18, 20, 22
 199 and 24 Aug 2018 (Figure 4). In house, the spectrum data were exported from the
 200 instrument by the Spectral Analysis and Management System software (HH2 Sync).
 201 The broadband albedo was calculated as a weighted average based on the spectral
 202 reflectance and the incoming solar radiation across the entire spectral wavelengths
 203 at each site (Ming et al., 2016; Moustafa et al., 2015; Wright et al., 2014; Yue et al.,
 204 2017). The period-mean albedo averaged for the 14 sites before and after
 205 conducting artificial-precipitation experiments (12 – 18 Aug and 18 – 24 Aug) are
 206 shown in Table 2. We excluded the apparent outliers (higher than 0.98) of the albedo
 207 data which are physically unrealistic.



208
 209 *Figure 4 The location of the AWS and the measuring sites for surface albedo and mass balance on*
 210 *the Muz Taw glacier.*

211

212 3.4 Measurement of the mass balance

213 We have measured the mass balance of the Muz Taw Glacier annually since 2014
 214 with the method introduced in Østrem and Brugman (1991). Metal stakes for mass-

215 balance measurements were fixed into the ice with a portable steam drill. The stake
216 network consisted of 23 stakes evenly distributed in different altitudes, where three
217 stakes in every row roughly (Figure 4). The stick scale for measuring balance was
218 read thrice, 12, 18 and 24 Aug, respectively. We compared the mass varying
219 between the two periods (12-18 Aug and 18-24 Aug). The snow depth at each stake
220 was measured by reading the scale, and the density of snow was measured by
221 weighing the mass of snow with a given volume. We used the depth and density
222 data of snow to calculate the mass balance at the stake sites. The mass balance
223 was obtained on 1 May and 31 Aug annually. For verifying the effect of artificial
224 snowfalls on the mass balance of the glacier, in particular, we conducted three
225 additional measurements for the mass balance on 12, 18 and 24 Aug 2018,
226 respectively. The baseline of all the mass balance data in this study is the mass
227 balance measured by the stakes on 12 Aug. The calculation of the mass balance of
228 the whole glacier is following an interpolated method based on singular-point
229 measurements introduced by Wang et al. (2014).

230

231 **4 Results and discussion**

232 **4.1 Natural or artificial precipitations and their amounts and forms**

233 Figure 5a shows the hourly temperature and precipitations recorded by the AWS
234 from 12 to 24 Aug 2018. There were some natural precipitations during 12 – 14 Aug,
235 while except this and that in the experiment days, the whole period of 12 – 24 Aug
236 was sparse in precipitations. Artificial-precipitation experiments were carried out on
237 19, 22 and 23 Aug. The amounts of precipitations were 6.2 mm on 19th, 1.3 mm on
238 20th, 1.8 mm on 22nd and 10.6 mm on 23rd, respectively. Most snowfalls were
239 observed during midnights and early mornings. It seems not likely to distinguish the
240 artificial precipitations from the natural ones if they were simultaneously mixed in all
241 these events.

242

243 Previous weather modification experiments using the same method as ours
244 concluded that it was challenging to tell that how much artificial precipitation mixed in
245 the whole amount directly came after conducting the cloud seeding (CSIRO, 1978;
246 Qiu and Cressey, 2008; Ryan and King, 1997). The results from the measurements
247 by Marcolli et al. (2016) and (Fisher et al., 2018) suggested the efficacy and success
248 of using AgI on growing ice nuclei in clouds and promoting snowfall. In our study,

249 there were significant precipitation amounts recorded by the AWS every single time
250 after we ignited the smoke generators, associated with a highly significant linear
251 relationship ($n = 10$, $r_2 = 0.9999$) between the timings of igniting Agl and recording
252 snowfalls (Figure 5b). The co-occurring of the significant snow falling using the Agl
253 smoke to seed cloud (Figure 3 and Figure 5b) allows supposing that we were
254 producing artificial precipitations.

255

256 The AWS at grassland in the forefield of the Muz Taw glacier was clear from the Agl
257 smoke during the AP experiments. This allows us to use the precipitation data
258 recorded by it as a control to distinguish natural precipitation from the artificial
259 recorded by the AWS at ELA. We lost the precipitation data from the AWS at
260 grassland during the first AP experiment on Aug 19 for the rain gauge was full and
261 overflowed. While for the second experiment, the precipitation data were
262 successfully collected from the AWS in the glacier's forefield for a comparison.

263

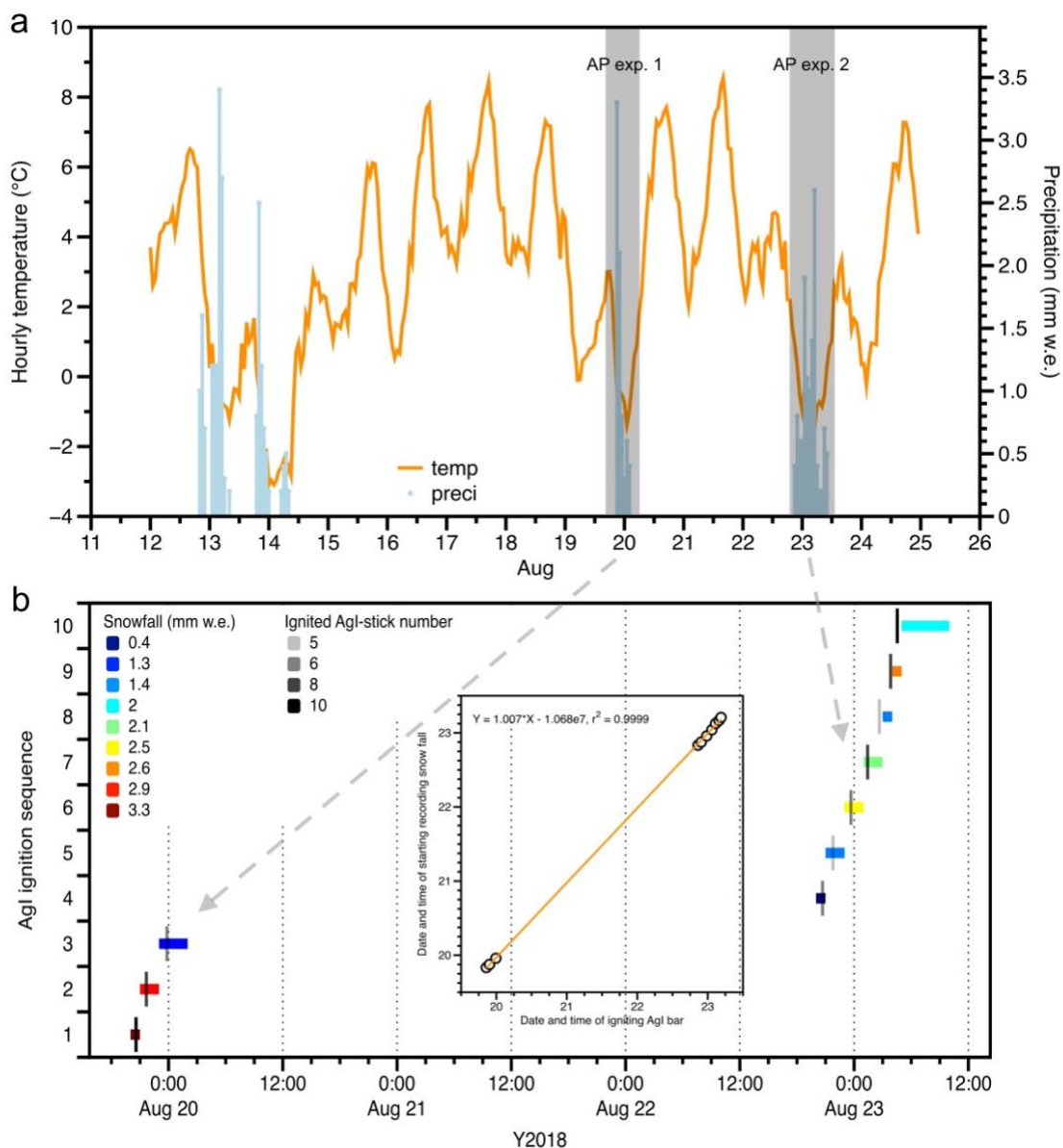
264 Figure 6 shows the precipitations recorded by both AWSs and the record ratio of
265 grassland to ELA during the second AP experiment (Aug 22 to 23). The
266 precipitations recorded by the two AWSs were not synchronized. The AWS at ELA
267 did not record any precipitations when that at grassland recorded at 19:00 and 20:00
268 on Aug 22; while there were records after 6:00 by the AWS at ELA but none for at
269 grassland. The correlation between the two precipitation records is fairly weak ($r_2 =$
270 0.05) when they were both recorded by the AWSs, implying that the cause of
271 precipitation (i.e. natural or artificial) might be distinctly different or likely mixed on
272 the target area.

273

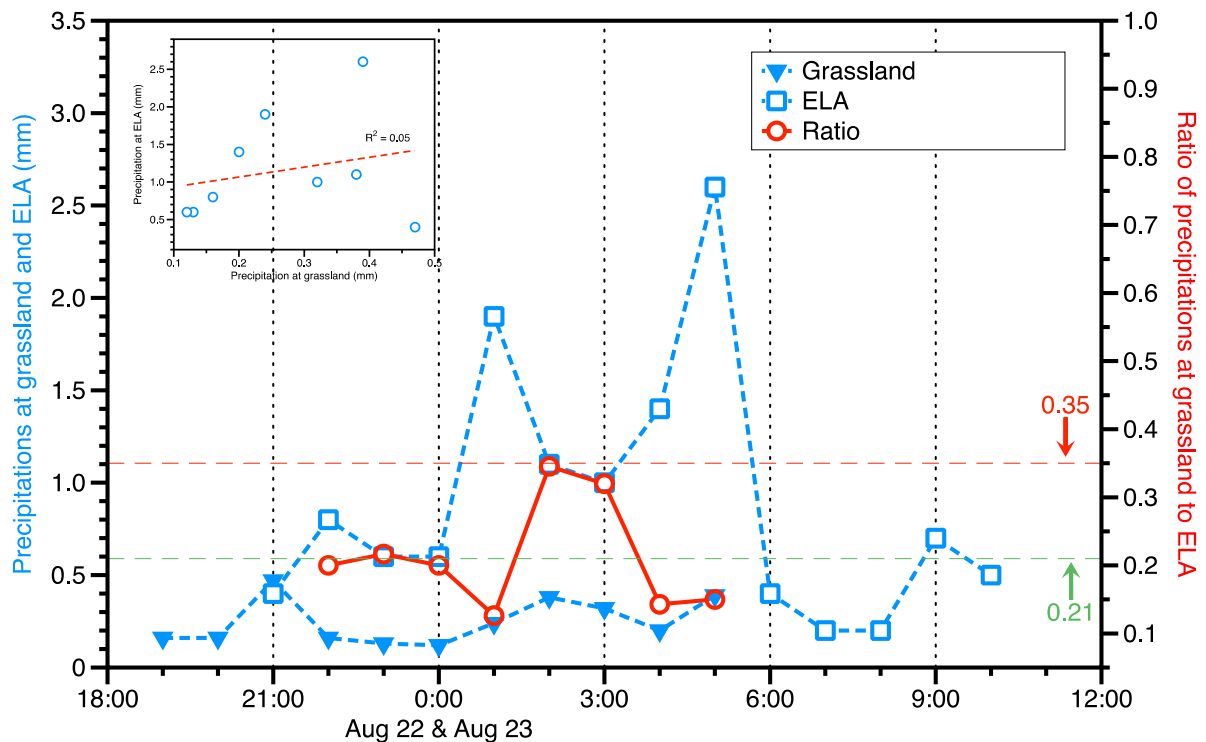
274 We presume two possibilities of whether there was natural precipitation joined the
275 artificial process targeted on the glacier. The first was none natural precipitation took
276 part in conceiving artificial snow on the target area, and the second, if any, was a
277 part of this. The ratios of precipitations by the AWS at the grassland to ELA were
278 smaller than 0.35 with a mean of 0.21 ± 0.03 (Figure 6), which could be used for
279 estimating how much naturally induced precipitation taking part in the AP experiment
280 based on the second presumption.

281

282 To determine the amount of solid precipitations that accumulates on the glacier
 283 surface, we apply a sinusoidal function (Möller et al., 2007) on the total precipitation.
 284 The function describes the transition between solid and liquid precipitations in a
 285 temperature range between +2 °C and +4 °C (Fujita and Ageta, 2000; Mölg et al.,
 286 2012). When the air temperature is lower than 2 °C, solid precipitations (snow) will
 287 occur, and between 2 – 4 °C rain would fall with snow. During our experiments, the
 288 air temperatures were below 2 °C when precipitations occur, implying that the
 289 precipitations in the two experiments were solid.



290
 291 *Figure 5 a) The daily snowfalls and hourly averaged temperature recorded by the AWS from 12 to 24*
 292 *Aug 2018, where the two artificial-precipitation experiments (AP exp. 1 and 2) are marked, and b) the*
 293 *hourly snowfall amounts (indicated by color) and time periods (indicated by length) recorded by the*
 294 *AWS and the ignited Agl-stick number (indicated by color) and time during the two experiments.*



295

296 *Figure 6 The precipitations recorded by the AWSs at grassland (inversed blue solid triangles) and*
 297 *ELA (hollow blue squares) and the precipitation-record ratio of grassland to ELA (hollow red circles)*
 298 *during Aug 22 to 23, in which the scatter plot of the precipitations by both AWSs is included and the*
 299 *green and red dashed lines indicate the upper limit and mean of the ratios.*

300

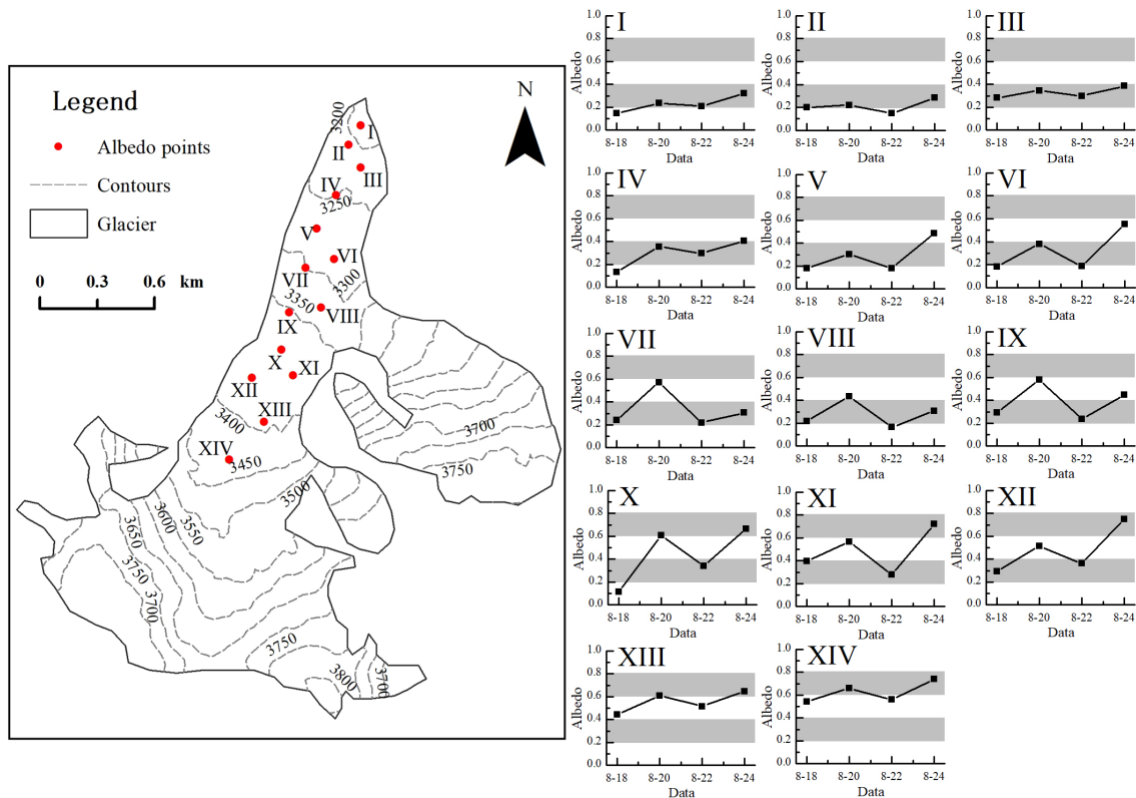
301 4.2 The effects of artificial snowfall on surface albedo

302 Glacier albedo is highly sensitive to snowfall. Once a snowfall occurs, it will quickly
 303 whiten the surface of the glacier and increase the albedo. Figure 7 shows the
 304 surface albedo of the Muz Taw Glacier at different locations before and after the
 305 artificial-snowfall experiments. We observed that the surface albedo at the sites
 306 varied from relative flatness (e.g., at site I and site III) to more significant fluctuations
 307 (e.g., at site XII and site VII) between 18 and 24 Aug.

308

309 Below 3250 m, the surface albedo (at sites I, II, III and IV) was generally smaller than
 310 0.4 (typical albedo of ice with debris) with mild fluctuations as shown in Figure 7.
 311 From 3250 to 3350 m a.s.l. (at sites V, VI, VII and VIII), significant variations in
 312 albedo were observed, ranging from 0.2 to 0.6. In the area of 3350-3400 m a.s.l.,
 313 more significant variations in albedo were observed between 0.1 and 0.7. Because
 314 this area was located near the equilibrium line, it was highly sensitive to air
 315 temperature and snowfall. Artificial snowfall frequently transited the surface from ice

316 to snow, and air temperature turned the surface inversely from snow to ice, and thus
 317 dramatic changes in albedo occurred. At sites XIII and XIV, which are much higher
 318 than the equilibrium line, the overall albedo exceeded 0.4 and rose up to 0.8. We
 319 observed a slightly increasing trend in albedo at these two sites (XIII and XIV),
 320 suggesting that the surface was covered by relatively lasting snow owing to artificial
 321 snowfalls.



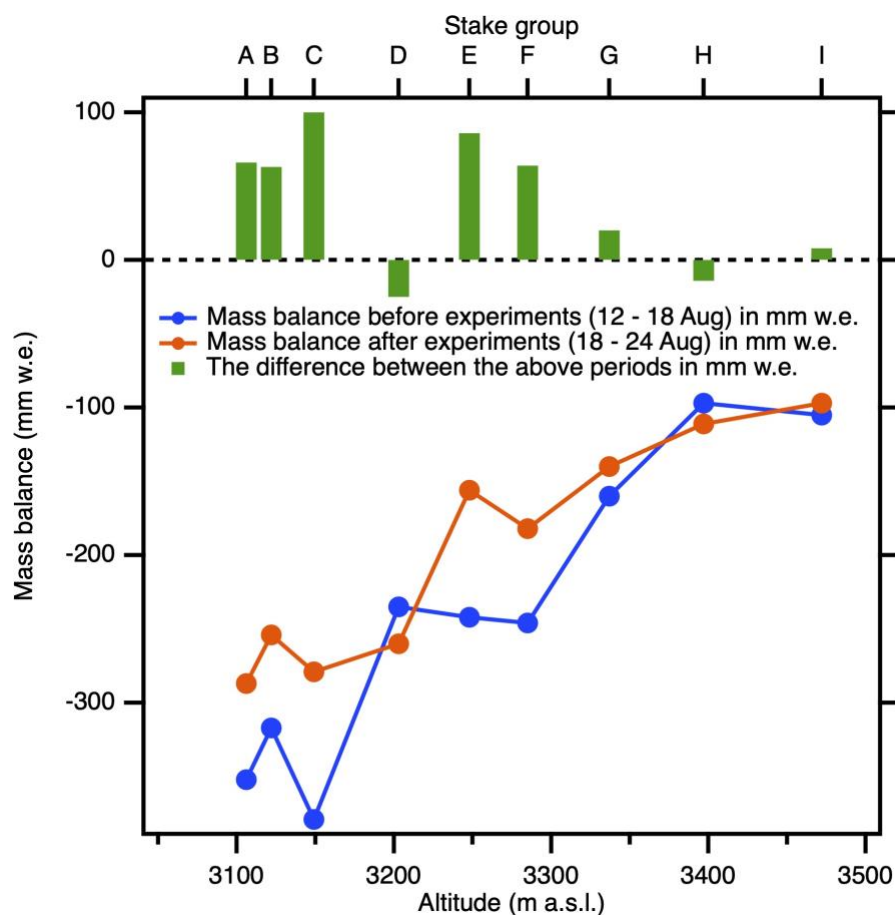
322
 323 *Figure 7 The surface albedo at the fourteen sites (I - XIV) of the Muz Taw Glacier, where the red*
 324 *points denote the sites and the top-left chart as the reference of the fourteen charts (site I to XIV)*
 325 *marks the albedo scale and date with the highlighted grey shades.*

326

327 4.3 The varying mass balance responding to the artificial snowfalls

328 As mentioned in Section 3.4, the stick scale for measuring balance was read thrice
 329 at each site, on 12, 18 and 24 Aug, respectively. To study the effects of the artificial
 330 snowfalls on the mass balance of the glacier, we calculated the mass balance
 331 measured by the stakes during the two periods, i.e. before the artificial snowfalls (12
 332 – 18 Aug) and after the artificial snowfalls (18 – 24 Aug), respectively. The stakes in
 333 a group (A to I) were roughly along the altitude contour (Figure 4), and the
 334 correspondingly measured mass balance of the same group was averaged (Figure
 335 8). The mass balance decrease with altitude from approx. – 400 mm w.e. at 3100 m

336 to approx. – 100 mm w.e. at the equilibrium line measured by the stakes before the
 337 artificial snowfalls, and decrease from approx. – 300 mm w.e. at 3100 m to approx. –
 338 100 mm w.e. at the equilibrium line after the artificial snowfalls. The difference of the
 339 mass balances measured at the sites between the two periods was 41 ± 15 mm w.e.
 340 averaged on the stake measurements for the Muz Taw Glacier, considering the
 341 difference was completely due to artificial precipitation. If we take 21% of the
 342 difference was due to natural precipitation (Figure 6), the difference would be 32 mm
 343 w.e. Therefore, the difference resulting from the artificial snowfalls accounted for
 344 14% (with 21% natural) to 17% (without natural) of the mass balance before the
 345 artificial snowfalls (- 237 mm w.e.).



346
 347 *Figure 8 The averaged mass balance measured at the sites (Stake A - I) before (blue) and after*
 348 *(orange) the artificial snowfalls on 18 and 20 Aug compared with that on 12 Aug (The zero line), and*
 349 *the gained mass (green = orange - blue) due to the artificial snowfalls.*

350

351 We compare the positively accumulative temperatures (in brief $PAT = \sum_{i=1}^n T_i$, n is
 352 the number of days, and T is the daily averaged temperature in $^{\circ}C$), the amounts of
 353 snowfalls, and the surface albedo of the measurements from 12 to 18 Aug (t_1) and

354 from 18 to 24 Aug (t_2) (Table 2), respectively. The two periods represent the same
 355 time-length span before and after the artificial snowfalls, respectively. The
 356 temperature, snowfall and albedo data in this comparison are all from the
 357 measurements of the AWS. The estimated mass balance after interpolating the
 358 measured mass balance by the stakes to the whole glacier during t_1 and t_2 were –
 359 61.4 mm w.e. and – 37.2 mm w.e., respectively. Although the PAT was higher during
 360 t_2 than during t_1 , the mass loss of the glacier was 40% lower than t_1 . More snowfall
 361 and higher albedo resulting from the artificial snowfalls can explain the less mass
 362 loss during t_2 .

363

364 *Table 2 The positive accumulated temperatures, snowfalls and albedo measured by the instruments*
 365 *on the AWS, and the calculated mass balance of the Muz Taw glacier during the two artificial-snowfall*
 366 *experiments ($t_1 = 12 - 18$ Aug, and $t_2 = 18 - 24$ Aug).*

| Period | Positively accumulated temperature (°C) | Snowfall (mm) | Albedo | Mass balance (mm) |
|--------|---|---------------|--------|-------------------|
| t_1 | 17.0 | 17.4 | 0.24 | - 61.4 |
| t_2 | 18.2 | 19.9 | 0.33 | - 37.2 |

367

368 The accumulation at the equilibrium line altitude (ELA) of a glacier is approximately
 369 equal to the area average of accumulation over the whole glacier (Braithwaite,
 370 2008). We can presume that the snowfall amount measured by the AWS near the
 371 ELA of the Muz Taw glacier during t_2 was the average received mass of the whole
 372 glacier after implementing the AP experiments. The extra melt amount from the
 373 glacier besides the gained mass during t_2 would be the difference between the
 374 calculated mass loss (37.2 mm w.e.) and the snow mass measured by the AWS
 375 (19.9 mm. w.e.), and that would be 17.3 mm w.e. The artificial snowfalls may
 376 significantly save the melt of the glacier by 54% during t_2 , calculated as the
 377 percentage of the snowfall divided by the estimated mass balance. Excluding 21% of
 378 the mass measured by the AWS presumably as the contribution of natural
 379 precipitations, we conclude that the artificial precipitations buffered the total melting
 380 during t_2 by 42%.

381

382 4.4 The mechanism: how artificial snowfalls reduce the melting of a glacier

383 In the air temperature lower than 2 °C, the artificial snowfall promotes the form of
384 snow which directly adds mass onto the glacier and increases the mass balance of
385 the glacier and thereby albedo; the snow cools the surface and increases the surface
386 albedo; the increased albedo will decrease the solar radiation absorption in the
387 surface and favour retaining the mass which will, in turn, save the albedo; and
388 eventually the whole process forms a positive feedback.

389
390 This is a very preliminary theory based on the limited data derived from the short-
391 term experiments, and we need further studies to validate the theory. The albedo
392 decay of artificial snowfall and snow physics are required to claim a long-term impact
393 on the mass balance of glaciers. Particularly, the variation in the likelihood of a
394 snowfall event occurring with or without smoke generators and the partition of natural
395 and artificial precipitations need to be quantified more confidently, for which more
396 controlling experiments are needed in future.

397

398 **5 Conclusions**

399 We used Agl-smoke generators to induce artificial snow on the Muz Taw Glacier in
400 Sawir Mountains on 19 and 22 Aug 2018. Two AWSs were set up on the target
401 glacier and control area, respectively. The albedo and mass balance were measured
402 at the stakes evenly distributed along the altitude contours of the glacier before and
403 after the artificial snowfall experiments. The glacier received a total snow amount of
404 ~ 20 mm w.e. by two experiments, which increased the surface albedo of the glacier.
405 Larger fluctuations in albedo were measured at the higher sites than lower.

406

407 By comparing the precipitations measured by the two AWSs, we conclude that
408 artificially induced snow could account for at least 79% of the total snow measured
409 by the AWS at the ELA. After interpolating the mass balance measured by the
410 stakes to the whole glacier, we get a mass balance of – 61 mm w.e. for the period of
411 12 – 18 Aug and – 37 mm w.e. for the period of 18 – 24 Aug, respectively. The
412 artificial snow reduced the mass loss of the glacier by ~ 40% due to more snowfall
413 and higher albedo, nevertheless the positively accumulated temperature during the
414 latter period was higher than the former.

415

416 We compared the mass balances directly calculated from the measurements of the
417 stakes before the experiments (12 – 18 Aug) with that after (18 – 24 Aug). The
418 difference between the two periods was 32 to 41 mm w.e., taking possible natural
419 snow into account. This suggests that artificial snow does add mass to the glacier,
420 which is consistent with the result by interpolating stake measurements to the whole
421 glacier. We also compared the total melt of the glacier during 18 – 24 Aug with the
422 artificial snow received by the glacier, implying that artificial snow significantly saved
423 the mass loss by 42% to 54% after the experiments.

424

425 We propose a theory describing the role of snowfall in reducing the melting of the
426 glacier. The mechanism determines that the environmental temperature and the form
427 of snowfall, and clouds are the two main factors resulting in the mass gain and loss
428 of a glacier. Mechanical erosion, energy exchange (thermal-dynamic) and albedo-
429 induced radiation absorption play major roles in the process of mass varying. This
430 hypothesized mechanism is preliminary and needs more measurements to
431 consolidate.

432

433 The approach in our work uses solar power to ignite the seeding material for forming
434 clouds and uses no extra water but redistributes natural water in the local
435 atmosphere at a small spatial scale. The energy-and-water saving techniques of the
436 approach with reasonably mass-loss-reducing efficiency from the Muz Taw glacier
437 validates its efficiency to possibly be applied in more Central-Asian glaciers to
438 reduce their rapid melting. Especially in summer when the melting is dramatic in the
439 Central-Asian glaciers, applying the approach suggested by our study on a much
440 broader scale might reduce the melting significantly. This study is preliminary and
441 short in operating time and needs more sophisticated experiments at control and
442 target areas to partition natural and artificial precipitations. The approach would
443 sophisticate itself when being implemented more regularly in future repeated and
444 longer-term, or scaled-up experiments.

445

446 **Code/Data availability**

447 It is currently shared by communities that the dataset would be publicly available
448 upon acceptance of publication. Please directly contact the corresponding author F.
449 Wang (wangfeiteng@lzb.ac.cn) or the coordinating author J. Ming

450 (petermingjing@hotmail.com) for the data repository and the authors will response
451 according to the statements.

452

453 **Author contributions**

454 F.W. conceived the main ideas, designed the experiment and drafted the
455 manuscript. X.Y., L.W., H.L. and Z.D. helped to design the experiment and collect
456 the data. J.M. reanalyzed the data and plots, edit the manuscript and sophisticated
457 the work.

458

459 **Competing interests**

460 All contributors declare no competing interests in this work.

461

462 **Acknowledgements**

463 The authors thank Samuel Morin and Suryanarayanan Balasubramanian for their
464 comments which are crucial for improving this work. This research is supported by
465 the Strategic Priority Research Program of the Chinese Academy of Sciences
466 (XDA20040501), the National Natural Science Foundation of China (41601076 and
467 41771081), the State Key Laboratory of Cryospheric Sciences (SKLCS-ZZ-2019)
468 and the Key Research Program of Frontier Sciences of Chinese Academy of
469 Sciences (QYZDB-SSW-SYS024).

470

471 **References**

472 Bojinski, S., Verstraete, M., Peterson, T. C., Richter, C., Simmons, A., and Zemp, M.:
473 The Concept of Essential Climate Variables in Support of Climate Research,
474 Applications, and Policy, B Am Meteorol Soc, 95, 1431-1443, 2014.

475 Bowen, E. G.: AUSTRALIAN EXPERIMENTS ON ARTIFICIAL STIMULATION OF
476 RAINFALL, Weather, 7, 204-209, 1952.

477 Braithwaite, R. J.: Temperature and precipitation climate at the equilibrium-line
478 altitude of glaciers expressed by the degree-day factor for melting snow, Journal of
479 Glaciology, 54, 437-444, 2008.

480 Council, N. R.: Critical Issues in Weather Modification Research, The National
481 Academies Press, Washington, DC, 2003.

482 CSIRO: Rainmaking; the state of the art. In: ECOS, 1978.

483 Dyer, C.: Now THAT'S a wrap! Swiss glacier is shrouded in UV-resistant blankets to
484 stop it melting in the summer heat. In: Daily Mail, Daily Mail, Online, 2019.

485 Fischer, A., Helfricht, K., and Stocker-Waldhuber, M.: Local reduction of decadal
486 glacier thickness loss through mass balance management in ski resorts, *The*
487 *Cryosphere*, 10, 2941-2952, 2016.

488 Fisher, J. M., Lytle, M. L., Kunkel, M. L., Blestrud, D. R., Dawson, N. W., Parkinson,
489 S. K., Edwards, R., and Benner, S. G.: Assessment of Ground-Based and Aerial
490 Cloud Seeding Using Trace Chemistry, *Advances in Meteorology*, 2018, 1-15, 2018.

491 Flossmann, A. I., Manton, M. J., Abshaev, A., Bruintjet, R., Murakami, M.,
492 Prabhakaran, T., and Yao, Z.: Peer Review Report on Global Precipitation
493 Enhancement Activities, 2018. 2018.

494 Fujita, K. and Ageta, Y.: Effect of summer accumulation on glacier mass balance on
495 the Tibetan Plateau revealed by mass-balance model, *Journal of Glaciology*, 46,
496 244-252, 2000.

497 Gerbaux, M., Spandre, P., George, E., and Morin, S.: Snow Reliability and Water
498 Availability for Snowmaking in the Ski resorts of the Isère Département (French
499 Alps), Under Current and Future Climate Conditions, *Journal of Alpine Research* |
500 *Revue de géographie alpine*, 2020. 2020.

501 Guo, W., Liu, S., Xu, J., Wu, L., Shanguan, D., Yao, X., Wei, J., Bao, W., Yu, P.,
502 and Liu, Q.: The second Chinese glacier inventory: data, methods and results,
503 *Journal of Glaciology*, 61, 357-372, 2015.

504 Hock, R., Rasul, G., Adler, C., Cáceres, B., Gruber, S., Hirabayashi, Y., Jackson, M.,
505 Kääb, A., Kang, S., Kutuzov, S., Milner, A., Molau, U., Morin, S., Orlove, B., and
506 Steltzer, H.: High Mountain Areas. In: IPCC Special Report on the Ocean and
507 Cryosphere in a Changing Climate, IPCC, New York, 2019.

508 Immerzeel, W. W., Lutz, A. F., Andrade, M., Bahl, A., Biemans, H., Bolch, T., Hyde,
509 S., Brumby, S., Davies, B. J., Elmore, A. C., Emmer, A., Feng, M., Fernández, A.,
510 Haritashya, U., Kargel, J. S., Koppes, M., Kraaijenbrink, P. D. A., Kulkarni, A. V.,
511 Mayewski, P., Nepal, S., Pacheco, P., Painter, T. H., Pellicciotti, F., Rajaram, H.,
512 Rupper, S., Sinisalo, A., Shrestha, A. B., Viviroli, D., Wada, Y., Xiao, C., Yao, T., and
513 Baillie, J. E. M.: Importance and vulnerability of the world's water towers, *Nature*, doi:
514 10.1038/s41586-019-1822-y, 2019. 2019.

515 Immerzeel, W. W., van Beek, L. P. H., and Bierkens, M. F. P.: Climate Change Will
516 Affect the Asian Water Towers, *Science*, 328, 1382-1385, 2010.

517 Kong, J., Wang, G., Fang, W., and Su, Z.: Laboratory study on nucleating properties
518 and microstructure of Agl pyrotechnics, *Meteorological Monthly*, 42, 74-79, 2016.

519 Marcolli, C., Nagare, B., Welti, A., and Lohmann, U.: Ice nucleation efficiency of Agl:
520 review and new insights, *Atmos Chem Phys*, 16, 8915-8937, 2016.

521 Ming, J., Xiao, C., Wang, F., Li, Z., and Li, Y.: Grey Tianshan Urumqi Glacier No.1
522 and light-absorbing impurities, *Environmental science and pollution research*
523 *international*, 23, 9549-9558, 2016.

524 Mölg, T., Maussion, F., Yang, W., and Scherer, D.: The footprint of Asian monsoon
525 dynamics in the mass and energy balance of a Tibetan glacier, *The Cryosphere*, 6,
526 1445-1461, 2012.

527 Möller, M., Schneider, C., and Kilian, R.: Glacier change and climate forcing in recent
528 decades at Gran Campo Nevado, southernmost Patagonia, *Annals of Glaciology*,
529 46, 136-144, 2007.

530 Moustafa, S., Rennermalm, A., Smith, L., Miller, M., Mioduszewski, J., Koenig, L.,
531 Hom, M., and Shuman, C.: Multi-modal albedo distributions in the ablation area of
532 the southwestern Greenland Ice Sheet, *The Cryosphere*, 9, 905-923, 2015.

533 Oerlemans, J., Haag, M., and Keller, F.: Slowing down the retreat of the Morteratsch
534 glacier, Switzerland, by artificially produced summer snow: a feasibility study,
535 *Climatic Change*, 145, 189-203, 2017.

536 Østrem, G. and Brugman, M.: Glacier mass-balance measurements: a manual for
537 field and office work, National Hydrology Research Institute, Inland Waters
538 Directorate Conservation and Protection Environment Canada, Saskatoon, Sask,
539 Canada, 224 pp., 1991.

540 Panagiotopoulos, F., Shahgedanova, M., Hannachi, A., and Stephenson, D. B.:
541 Observed Trends and Teleconnections of the Siberian High: A Recently Declining
542 Center of Action, *J Climate*, 18, 1411-1422, 2005.

543 Qiu, J. and Cressey, D.: Meteorology: Taming the sky, *Nature*, 453, 970-974, 2008.

544 Ryan, B. F. and King, W. D.: A Critical Review of the Australian Experience in Cloud
545 Seeding, *B Am Meteorol Soc*, 78, 239-254, 1997.

546 Silverman, B. A.: A Critical Assessment of Glaciogenic Seeding of Convective
547 Clouds for Rainfall Enhancement, *B Am Meteorol Soc*, 82, 903-924, 2001.

548 Smith, E. L.: Cloud seeding experiments in Australia, 1967.

549 Song, L.: Blue book on climate change in China, Center on Climate Change Press,
550 2019.

551 Vonnegut, B.: The Nucleation of Ice Formation by Silver Iodide, *Journal of Applied*
552 *Physics*, 18, 593-595, 1947.

553 Wang, F., Xu, C., Li, Z., Anjum, M. N., and Wang, L.: Applicability of an ultra-long-
554 range terrestrial laser scanner to monitor the mass balance of Muz Taw Glacier,
555 Sawir Mountains, China, *Sciences in Cold and Arid Regions*, 10, 0047-0054, 2018.

556 Wang, P., Li, Z., Li, H., Wang, W., and Yao, H.: Comparison of glaciological and
557 geodetic mass balance at Urumqi Glacier No. 1, Tian Shan, Central Asia, *Global*
558 *Planet Change*, 114, 14-22, 2014.

559 Wang, Y. Q., Zhao, J., Li, Z. Q., and Zhang, M. J.: Glacier changes in the Sawuer
560 Mountain during 1977-2017 and their response to climate change, *Journal of Natural*
561 *Resources (in Chinese)*, 34, 802-814, 2019.

562 Wright, P., Bergin, M., Dibb, J., Lefer, B., Domine, F., Carman, T., Carmagnola, C.,
563 Dumont, M., Courville, Z., and Schaaf, C.: Comparing MODIS daily snow albedo to
564 spectral albedo field measurements in Central Greenland, *Remote Sens Environ*,
565 140, 118-129, 2014.

566 Xu, Z., Jing, H., Zou, L., and Li, Y.: Application research of type WR-08X digital radar
567 on artificial precipitation in Saur Mountains area, *Jiangxi Science (in Chinese)*, 35,
568 727-730, 2017.

569 Yue, X., Zhao, J. U. N., Li, Z., Zhang, M., Fan, J. I. N., Wang, L. I. N., and Wang, P.:
570 Spatial and temporal variations of the surface albedo and other factors influencing
571 Urumqi Glacier No. 1 in Tien Shan, China, *Journal of Glaciology*, 63, 899-911, 2017.

572 Zemp, M., Huss, M., Thibert, E., Eckert, N., McNabb, R., Huber, J., Barandun, M.,
573 Machguth, H., Nussbaumer, S. U., Gartner-Roer, I., Thomson, L., Paul, F.,
574 Maussion, F., Kutuzov, S., and Cogley, J. G.: Global glacier mass changes and their
575 contributions to sea-level rise from 1961 to 2016, *Nature*, 568, 382-386, 2019.

576

577